Finite Element Analysis of the Loop Test Method for Stent Radial Force Characterization

Draft Report
November 9, 2004

Prepared by

ECHOBIO LLC
3557 Pleasant Beach Drive
Bainbridge Island, WA 98110
(206) 780-0750

Prepared for

CONFIDENTIAL

Contents

List of Figures

1 Objective

Develop base models for three representative balloon expandable stent geometries and determine the radial force characteristics using Finite Element Analysis (FEA). Develop analysis methodology to simulate two typical test methods for characterizing radial force, compare numerical simulation results to experimental results for the three representative expandable stent geometries and critically evaluate both test methods by systematically exploring key experimental factors.

The purpose of this work is to develop a rigorous experimental and numerical approach to characterize the radial response of balloon expandable and self-expanding stents. Here we focus our attention on the Loop Test Method to explore the sensitivity of the results to key experimental parameters.

2 Introduction

The ASTM F04.30.06 sub-committee is currently developing standards to address the radial force characteristics of stents. Three representative geometries (shown in Figure 1) are being considered and have been used as prototypes for round robbin testing at various laboratories. Two types of tests were employed in the initial round robbin.

The first test method (Concentric Cylinder Test Method) employs a visually clear, small diameter tube within a second slightly larger concentric tube. The stent is catheter deployed inside the first tube. Subsequently, the pressure between the first and second tubes is increased monotonically while monitoring the diameter of the first tube. The result is a plot of applied pressure between the concentric tubes versus stent diameter computed from the outer diameter of the inner tube.

The second test method (Loop Test Method) employs a thin strap (or loop) that circumferentially surrounds the stent and passes through a pair of closely spaced rollers. The strap is fixed at one end and the other end is pulled linearly so that the length of the strap surrounding the stent becomes smaller. The force required to pull the strap and the change in diameter are monitored throughout the test and the result is a plot of loop force versus stent diameter.

The following conclusions can be drawn from the initial round robbin testing:

- The three different stent geometries resulted in consistent and anticipated trends of measured effective radial force characteristics
- Significant scatter existed between tests of the same geometry within a given laboratory
- Significant scatter existed between tests of the same geometry between various laboratories
- Despite fairly good agreement between results for Parts 2 and 3 between the experimental work performed at W.L. Gore and Cordis, no definitive comparison can be made between the results produced using the Concentric Cylinder Test Method and the Loop Test Method.

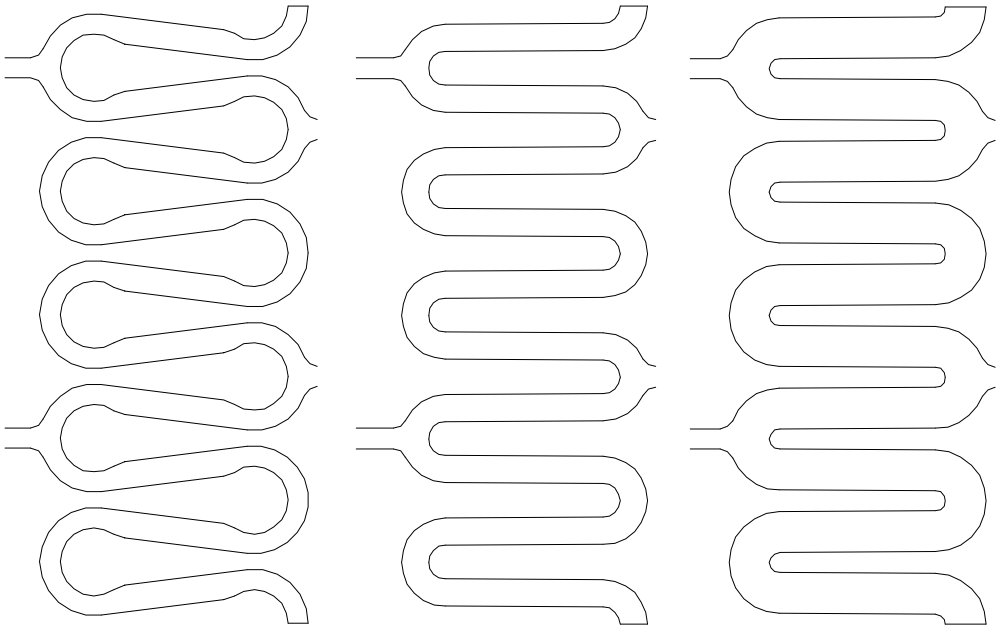

Figure 1: Schematic of the three stent geometries used in this work.

3 FEA "Ideal" Radial Force Analysis

The analyses are performed using the commercial finite element code ABAQUS/Standard. A variety of pre- and post-processing software tools are used to build the models, analyze the data and verify the results. The FEA models took advantage of symmetry of the design and only a single strut was considered in the analyses. The models were created by inscribing elements within the 2D geometry, extruding these elements through their thickness and wrapping these 3D elements around the longitudinal axis of the component. The finite element models were scanned for redundant node, element, connectivity and aspect ratio errors, and converted into cylindrical coordinates prior to performing the analyses.

A simple elasto-plastic material model was used for comparison between the three designs and is shown in Figure 2. The parameters for this model were calibrated per the specifications for the material used to manufacture the stents.

Boundary conditions were applied to the base models that constrained rigid body motions and that were consistent with the symmetry cutting planes. Additional contact constraints were included to simulate the balloon expansion and subsequent radial loading of the stent. This was accomplished using an analytically defined expanding rigid cylinder with softened contact between the cylinders and the surfaces of the stent strut. All three stent were expanded to the same peak inner diameter and allowed to recoil and no attempt was made here to match the final recoiled diameters of the stents. Additional simplifications include zero friction between the stent surface and the rigid cylinder.

Figures 3 and 4 show contour plots of the vonMises stress for the geometry of stent 1 at peak diameter during balloon expansion and after recoil, respectively. Figures 5 and 6, and 7 and 8 show similar plots for the geometries of stents 2 and 3, respectively. Note that although both tensile and compressive stresses occur in the parts, the vonMises stress is a positive measure of effective stress.

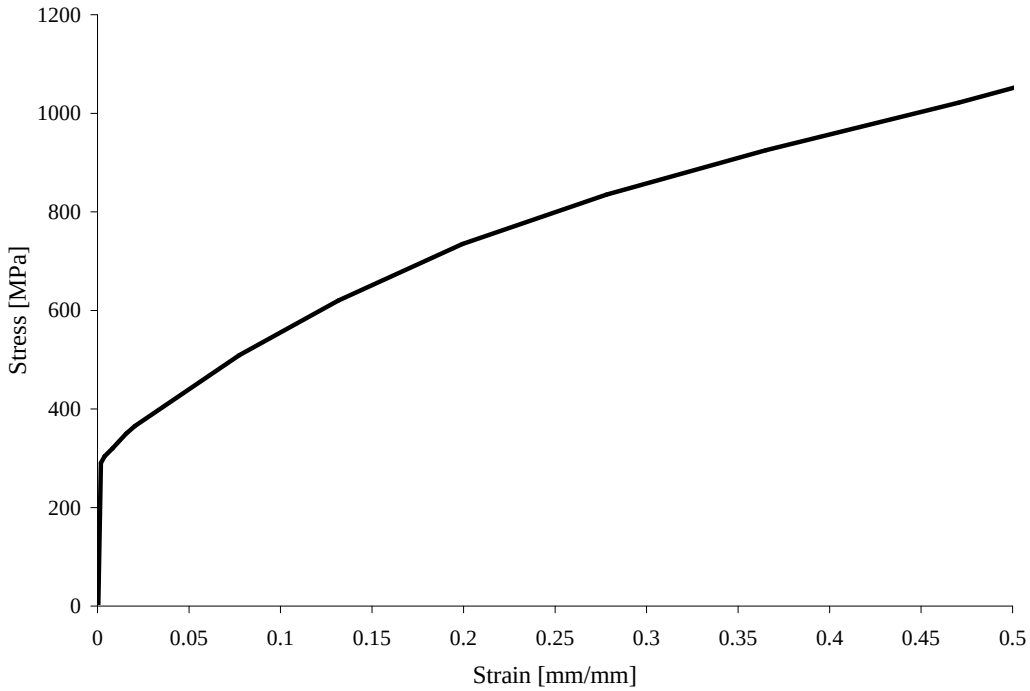

Figure 2: Material model used in the analyses.

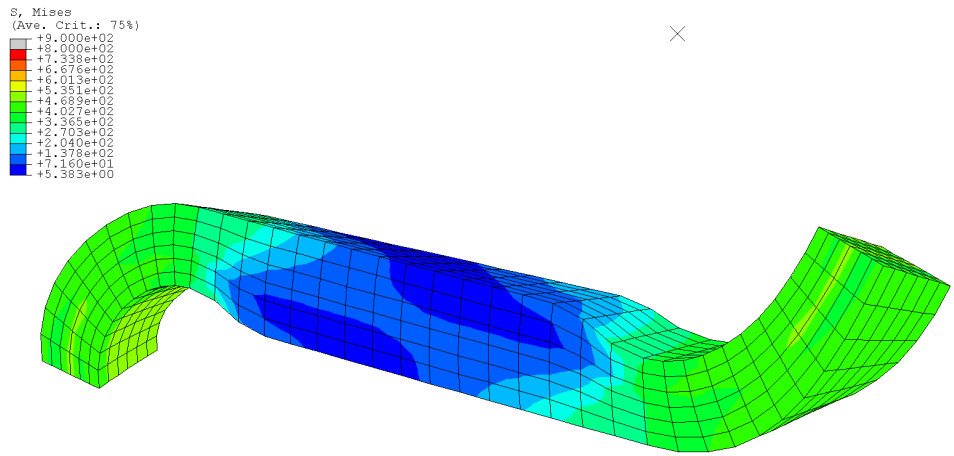

Figure 3: Contour plot of the vonMises stress at peak expanded diameter for Stent 1.

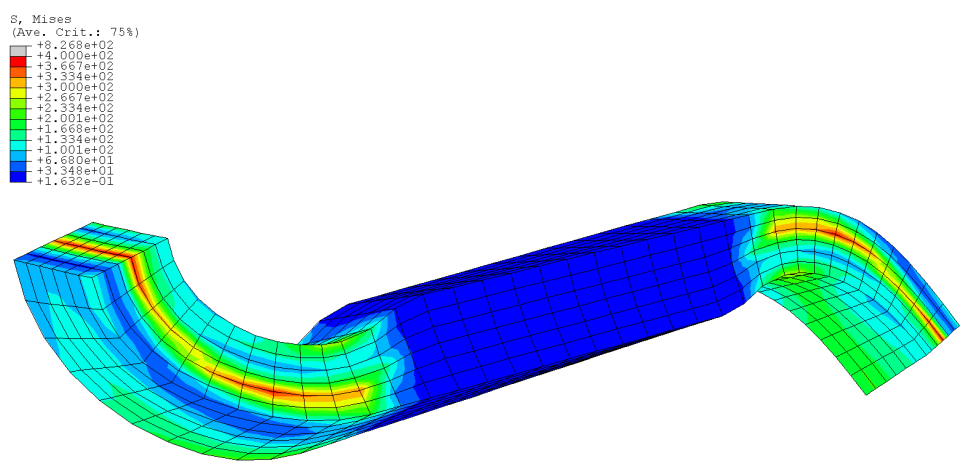

Figure 4: Contour plot of the vonMises stress after recoil for Stent 1.

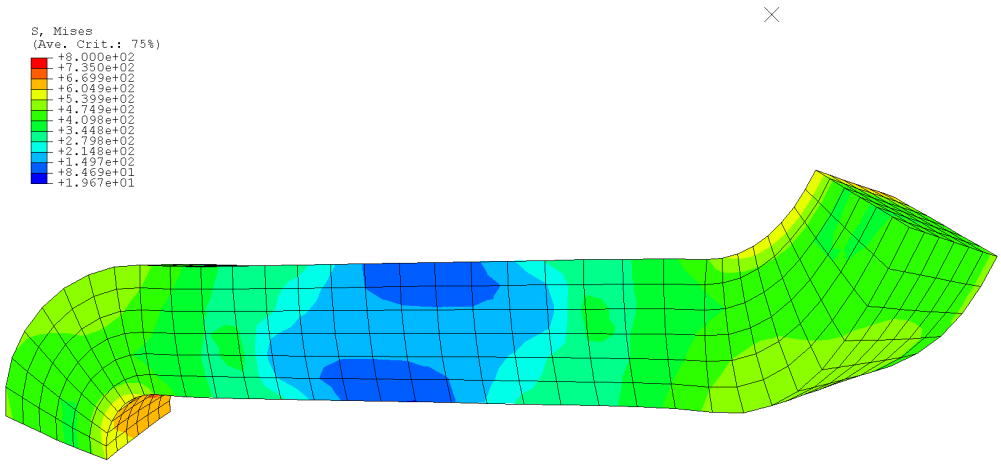

Figure 5: Contour plot of the vonMises stress at peak expanded diameter for Stent 2.

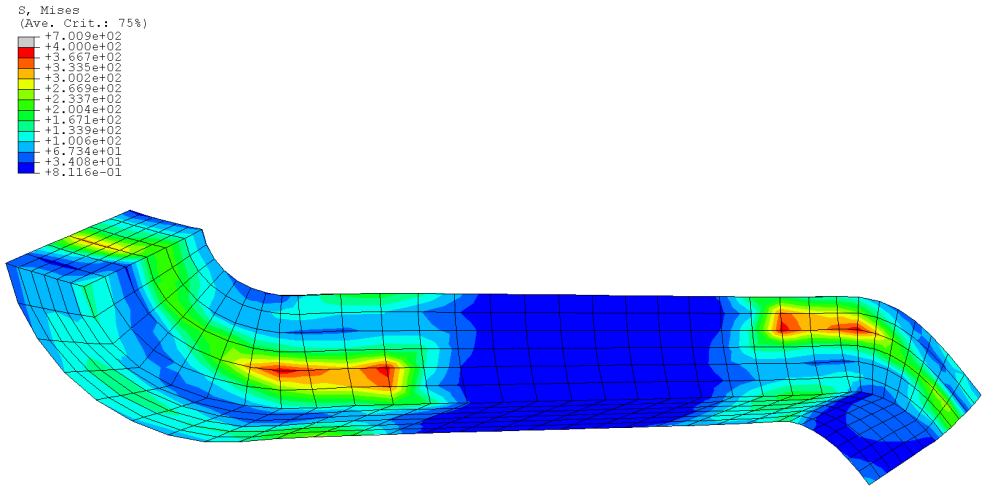

Figure 6: Contour plot of the vonMises stress after recoil for Stent 2.

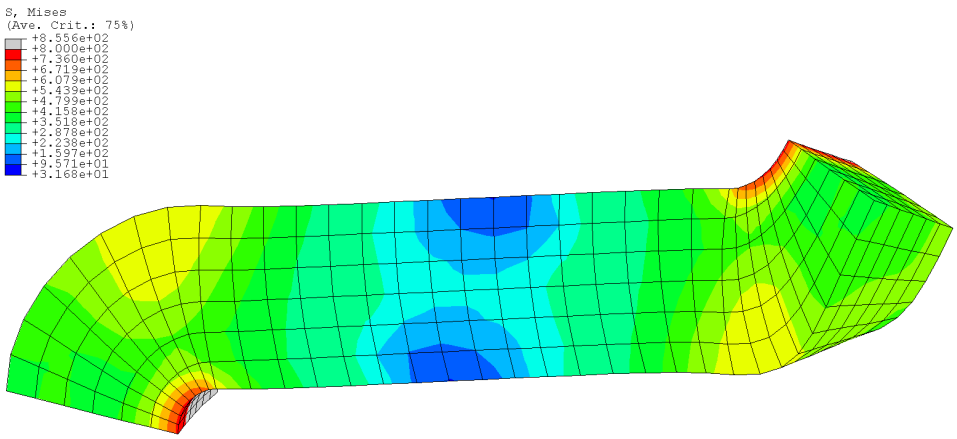

Figure 7: Contour plot of the vonMises stress at peak expanded diameter for Stent 3.

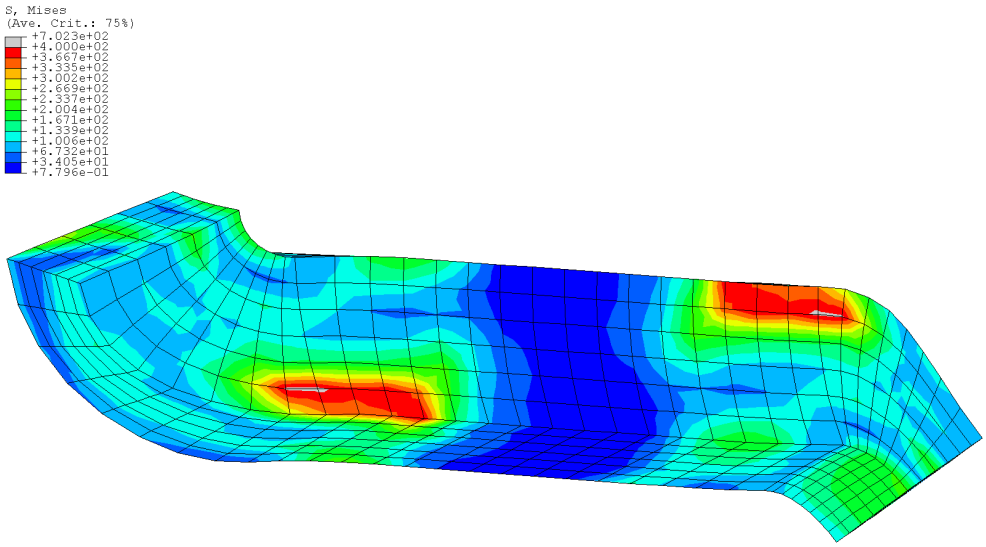

Figure 8: Contour plot of the vonMises stress after recoil for Stent 3.

3.1 "Ideal" Radial Force Analysis Results

The contact force between the rigid cylinder and the surface of the stent can be readily computed throughout the analyses. This force represents the radial force component (in cylindrical coordinates) exerted by a single strut. Figure 9 shows the Force per strut (in Newtons) versus radial displacement (in millimeters) during the balloon expansion and recoil for the three stent geometries. The plot indicates that during expansion, the three stents experience significant plastic deformation followed by minimal elastic unloading during recoil and that the three designs have significantly different radial force characteristics.

Subsequent to balloon expansion, the stents were loaded with another analytically defined contracting rigid cylinder that simulated the inward radial loading of the stent. Figure 10 shows the Force per strut (in Newtons) versus radial displacement (in millimeters) during the inward radial loading for the three stent geometries.

Note these results represent the idealized case of a uniformly expanded and contracted stent and as such are not directly comparable to the results obtained from either the loop test or concentric cylinder test method. This is obvious in Figure 11 which shows the experimental results for the three representative stent geometries using the Loop Test Method with the ideal radial force calculations using FEA.

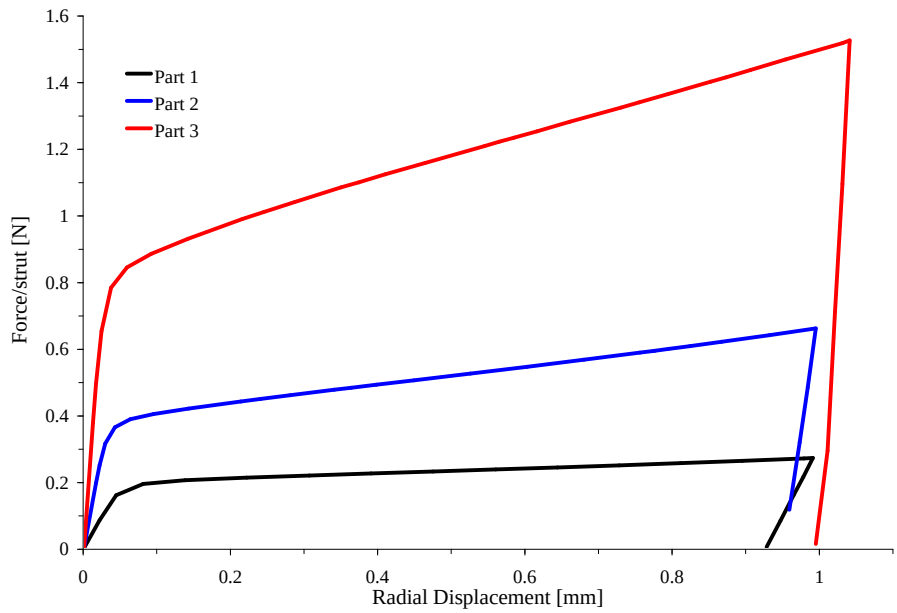

Figure 9: Force/strut as a function of radial displacement during expansion and recoil for the three stent geometries.

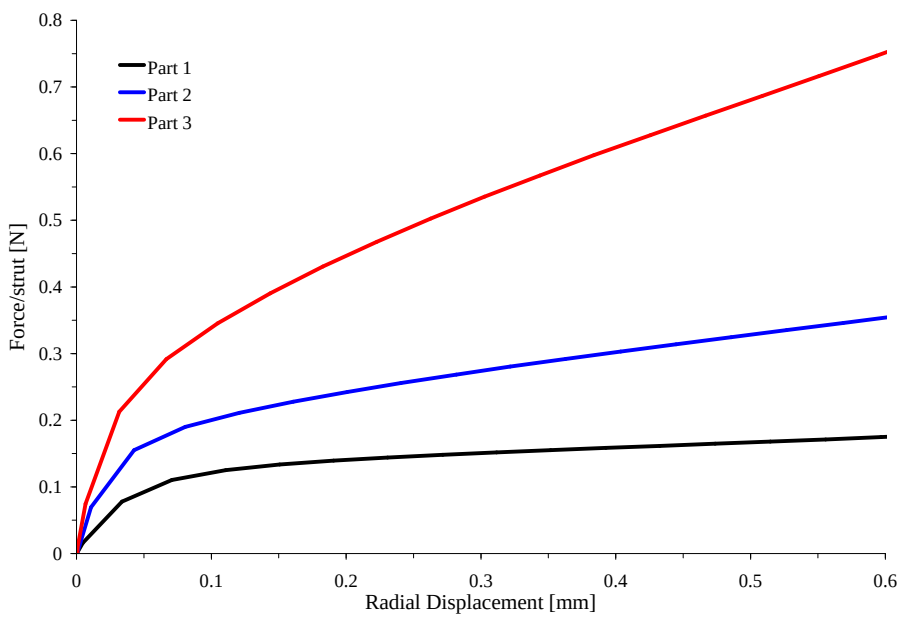

Figure 10: Force/strut as a function of radial displacement during inward radial loading of the three stent geometries.

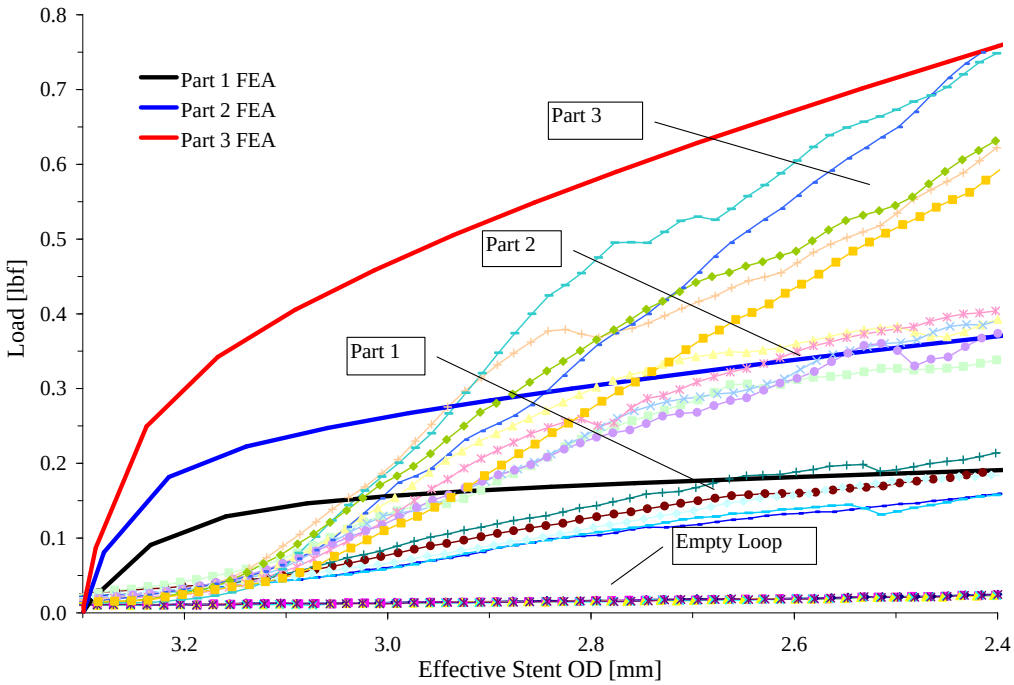

Figure 11: Comparison of the experimental results for the three representative stent geometries using the Loop Test Method with the ideal radial force calculations using FEA (denoted by the solid lines).

4 FEA Loop Test Method Analysis

The loop test as applied to stent 2 was simulated using FEA. Here, one half of the a row of struts was modeled (the other half was omitted due to symmetry) along with the loop as shown in Figure 12. Boundary conditions were applied to the stent model that constrained rigid body motions and that were consistent with the symmetry cutting planes of the stent. Additional symmetry conditions were applied to the loop strap model that were consistent with symmetry planes on the two curved sides as well as the fixed side of the loop. Prescribed displacement boundary conditions were applied to one end of the loop that are meant to be representative of actually pulling on the end of the loop strap. In order to obtain the expanded geometry for the stent, the stent was expanded as per the idealized methodology using an analytically defined expanding cylinder as described previously. Figure 13 shows a contour plot of the vonMises stress after recoil for the model used on the loop test analyses.

Key parameters that were varied included the coefficient of friction between the loop and the surface of the stent ($0.05 < \mu < 0.2$), loop material stiffness ($50\,\mathrm{MPa} < E < 5\,\mathrm{GPa}$)and loop thickness ($0.05\,\mathrm{mm} < t < 0.2\,\mathrm{mm}$). Note that this still represents a certain degree of simplification in the model as no attempt was made to model the closely spaced rollers (along with their corresponding frictional effects) as well as stent–end and loop–end effects.

Figures 14 and 15 show the deformed meshes for simulations of the loop test where a large coefficient of friction and a small coefficient of friction was assumed between the loop strap and the surface of the stent. Note that in the case of a large coefficient of friction, friction causes the stent to be pulled around with the relative motion of the loop strap resulting in excessive deformation of the struts close to the roller section of the test. Whereas in the case of a small coefficient of friction, more uniform loading of the stent is obtained and no bunching occurs where the loop strap is being pulled.

Figures 16 and 17 show the deformed meshes for simulations of the loop test where the loop was considered to be relatively stiff and relatively thin, respectively. Note that in the case of a stiff loop, the loop strap remains more cylindrical as the end of the strap is pulled, whereas the thin strap conforms more easily to the surface of the stent. This is indicative of significant nonuniform loop stretching during the analysis.

Figures 18 and 19 show the effective pressure distribution in the loop representing the pressure generated by the stent at two stages during the loop test simulation. Figures 20 and 21 show contour plots of the vonMises stress in the stent at two stages during the loop test simulation. Note that although the magnitude of the stress in the stent increases during the loop test analysis, the magnitude of the peak pressures (magnitude of the red areas) in Figures 18 and 19 remain relatively constant but increase significantly in size during the loop test analysis. Lastly, Figures 22 and 23 show contour plots of the vonMises stress in the stents 1 and 3 during the loop test simulation.

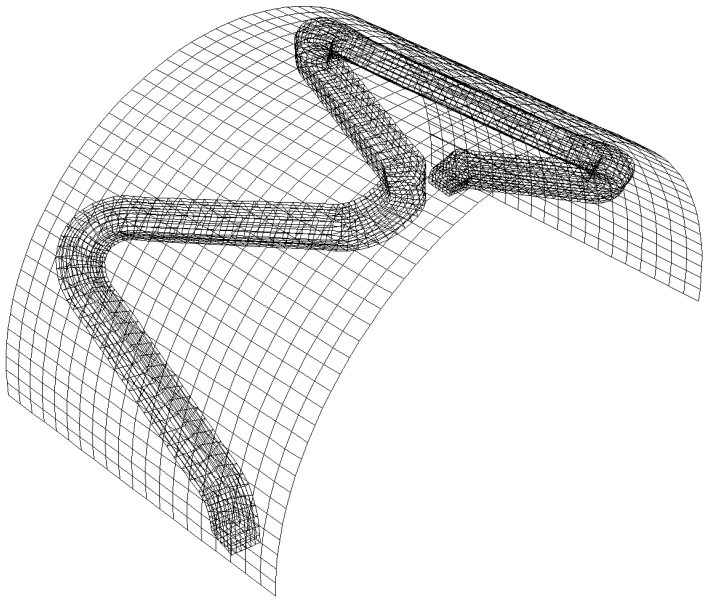

Figure 12: Schematic and meshes of the loop and stent geometry used to simulate the Loop Test Method.

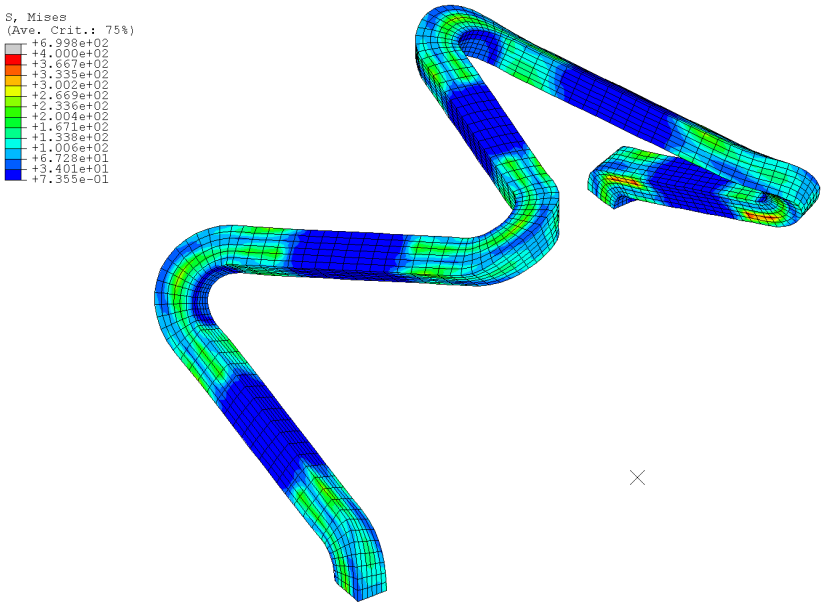

Figure 13: Contour plot of the vonMises stress after recoil for the model of Stent 2 used in the loop test simulations

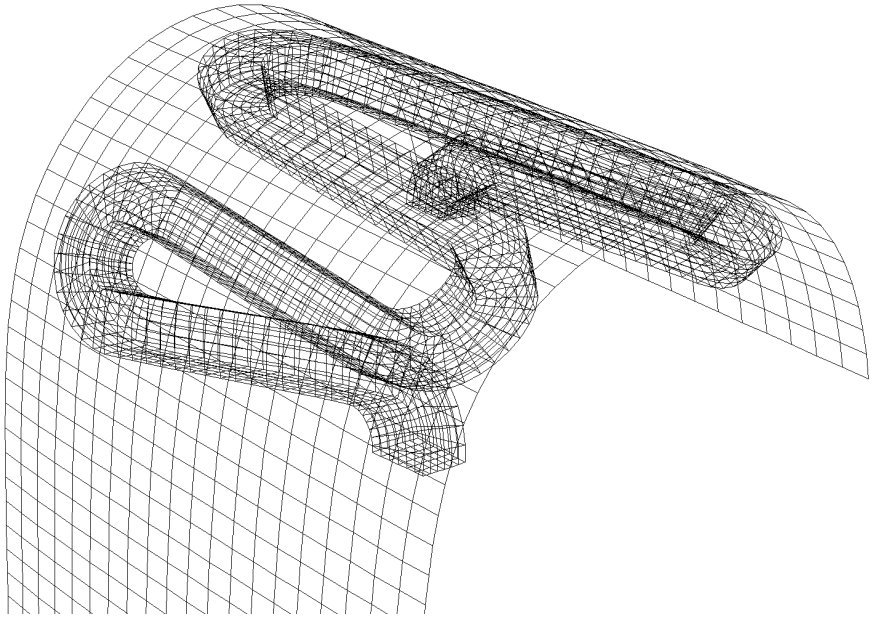

Figure 14: Demonstration of the effect of a large coefficient of friction between the stent and loop strap.

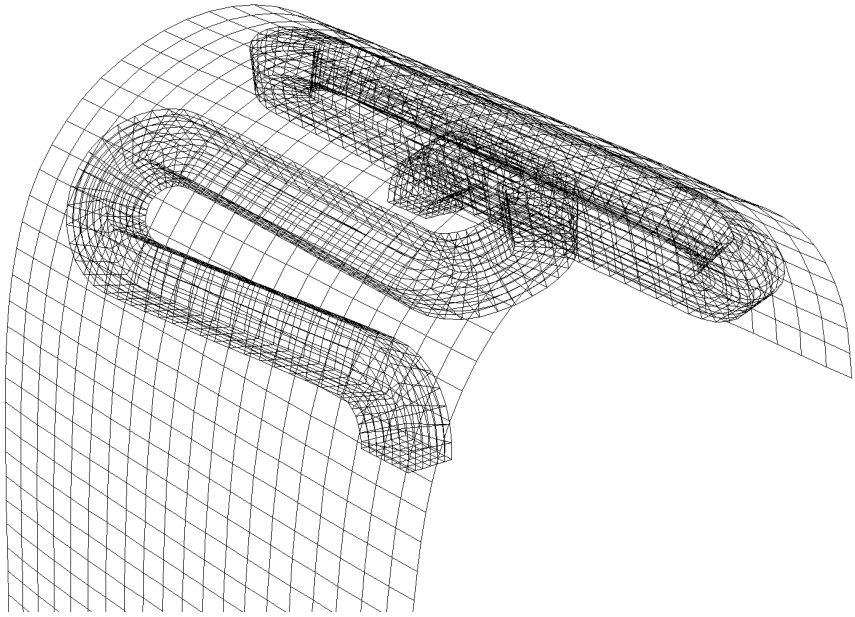

Figure 15: Demonstration of the effect of a small coefficient of friction between the stent and loop strap.

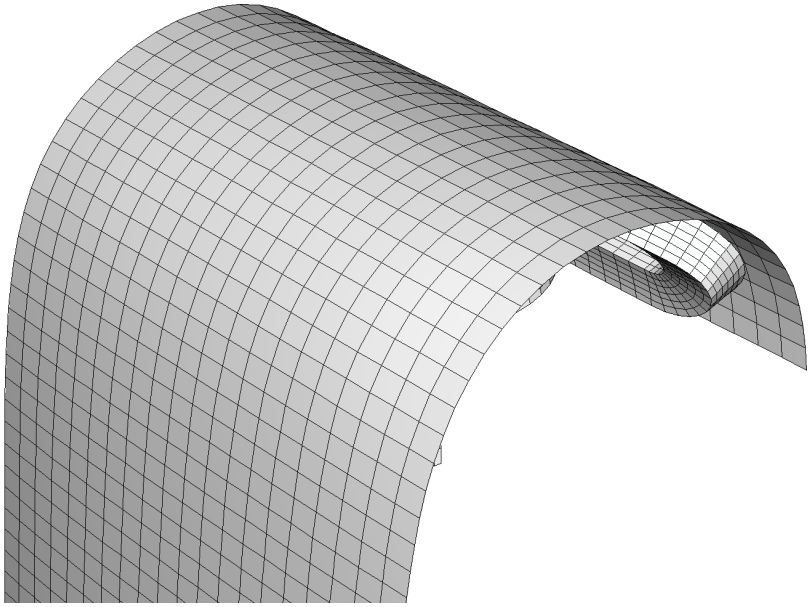

Figure 16: Demonstration of the effect of a stiff strap in the Loop Test Method.

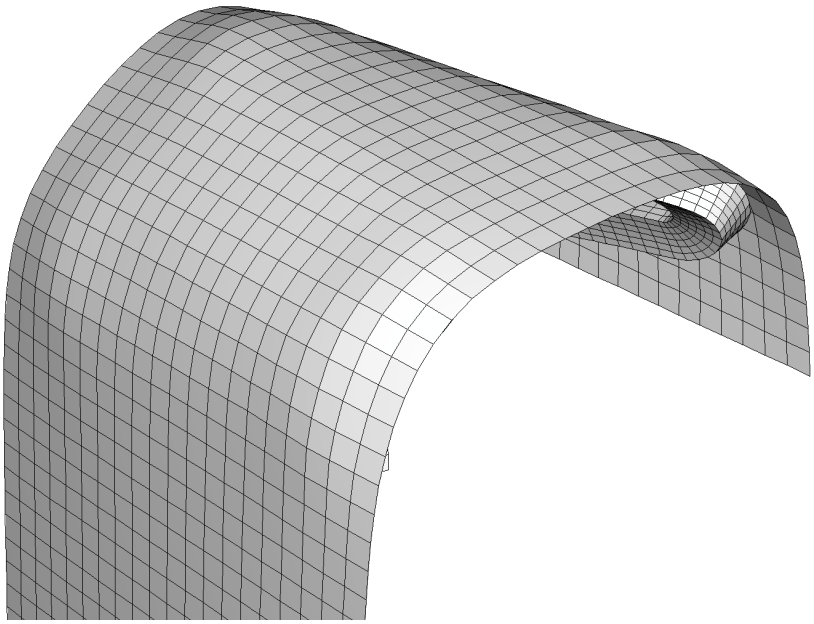

Figure 17: Demonstration of the effect of a more compliant strap in the Loop Test Method.

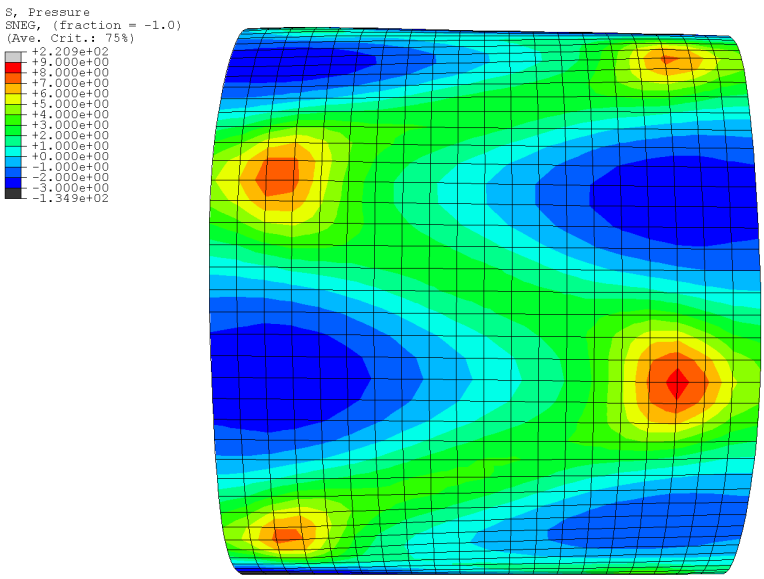

Figure 18: Contour plot of pressure on the strap at an intermediate loading.

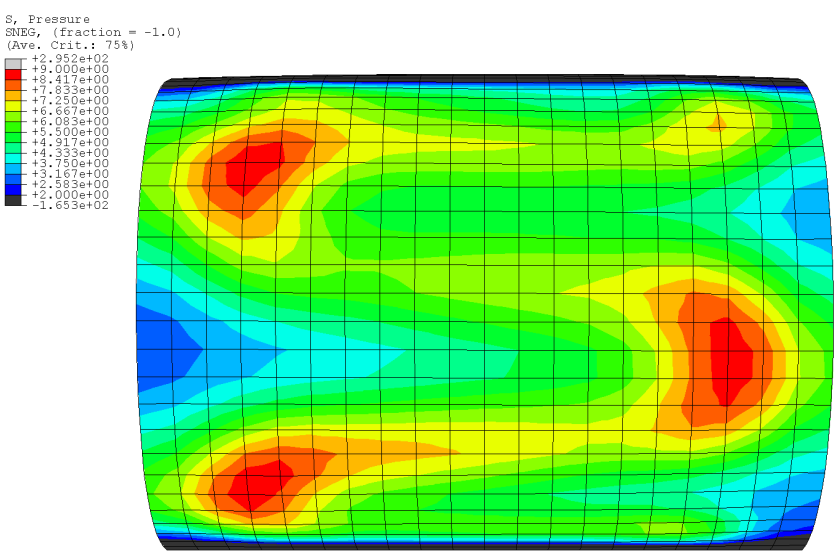

Figure 19: Contour plot of pressure on the strap at a maximum loading.

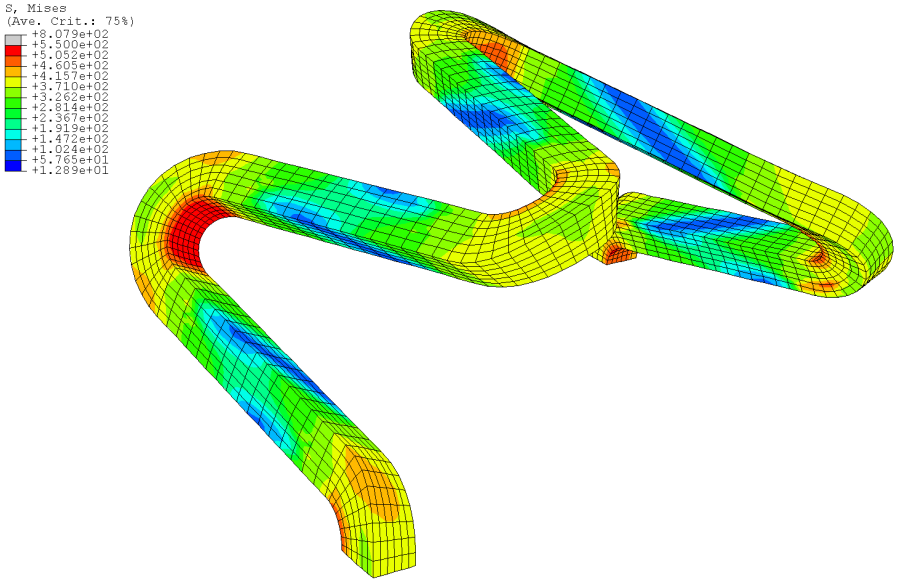

Figure 20: Contour plot of the vonMises stress in the stent at an intermediate loading.

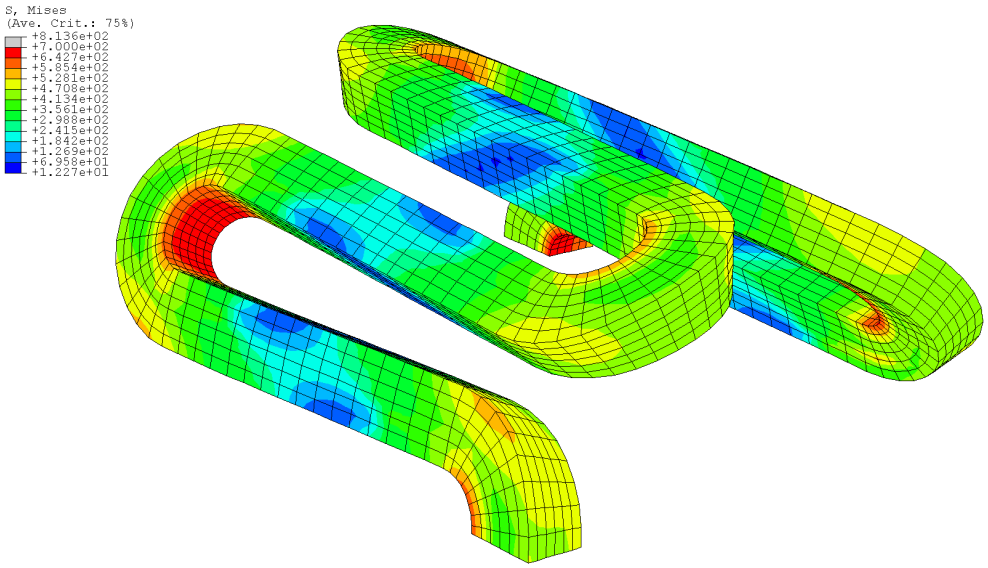

Figure 21: Contour plot of the vonMises stress in Stent 2 at maximum loading.

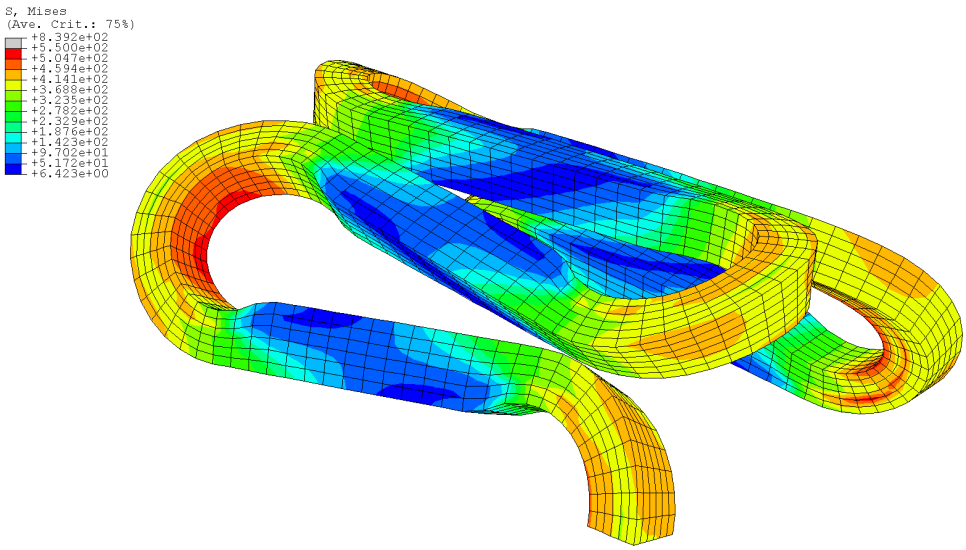

Figure 22: Contour plot of the vonMises stress in Stent 1 during the loop test.

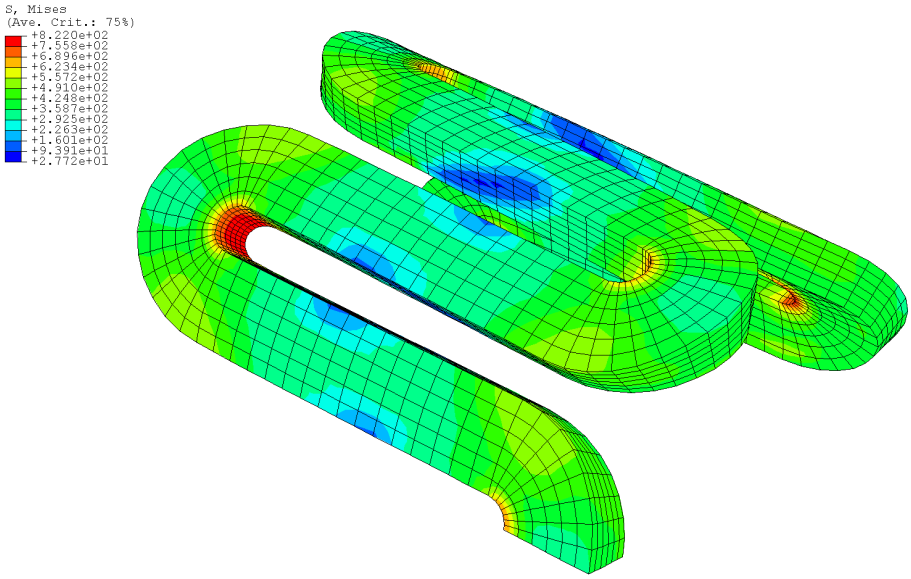

Figure 23: Contour plot of the vonMises stress in Stent 3 during the loop test.

4.1 FEA Loop Test Method Radial Force Results

The loop test analysis can be used to explore the influence of key parameters such as friction, loop material stiffness and loop thickness on the measured response during the loop test. Figure 24 attempts to show the range of possible responses that can be obtained by varying the parameters of the loop test analysis. Nine different combinations of the key parameters were considered and it is clear that significantly different results than the ideal radial force case (denoted by the solid black line) can be obtained. In order to make sense of these results, consider the effect of each key parameter separately.

4.1.1 Influence of loop stiffness

Figure 25 shows the effect of loop strap material stiffness on the load versus effective stent diameter response. The stiffness of the loop has a significant impact on the response during the initial stages of the loop test. In the case of a low stiffness loop, the added loop compliance allows the loop to conform to the surface of the stent thereby softening (reducing) the measured force. As the analysis proceeds, the relative differences between the three cases decreases.

4.1.2 Influence of loop thickness

Figure 26 shows the effect of loop strap thickness on the load versus effective stent diameter response. The thickness of the loop has a significant impact on the response during the initial stages of the loop test and as one would expect, in the same fashion as loop stiffness. Again, as the analysis proceeds, the relative differences between the three cases decreases.

4.1.3 Influence of friction between the loop and stent

Figure 27 shows the effect of friction between the loop strap and the surface of the stent on the load versus effective stent diameter response. Plotted are the results for two different strap thicknesses. In both cases, higher friction results in a decrease in the force with effective stent diameter. The influence is small at the start of the analysis and the effect increases as the analysis proceed, which is as one would expect.

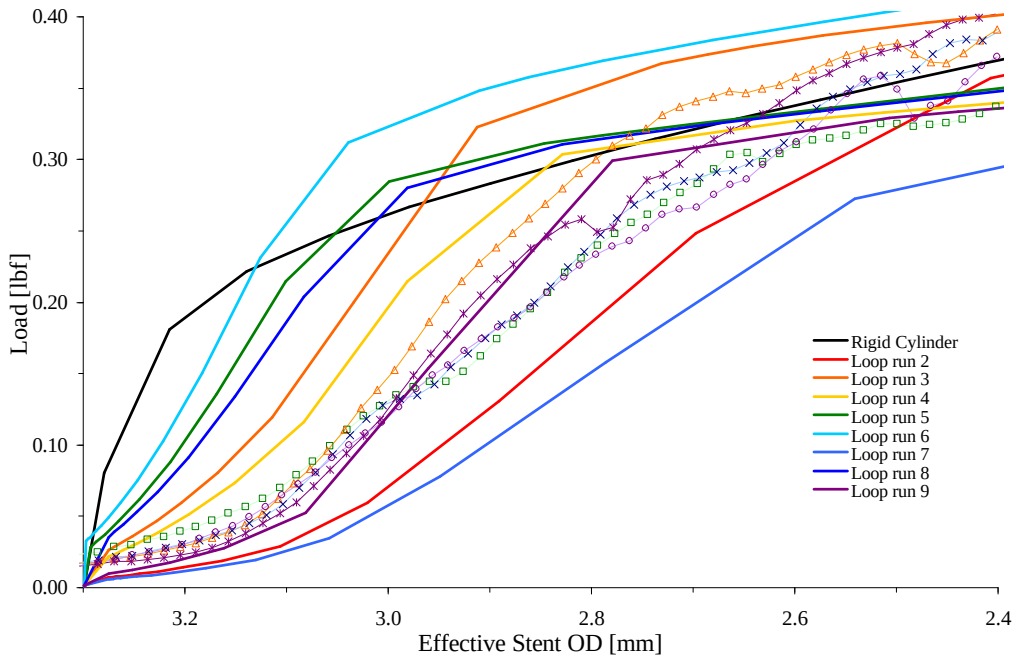

Figure 24: Experimental and parametric FEA results for Stent 2.

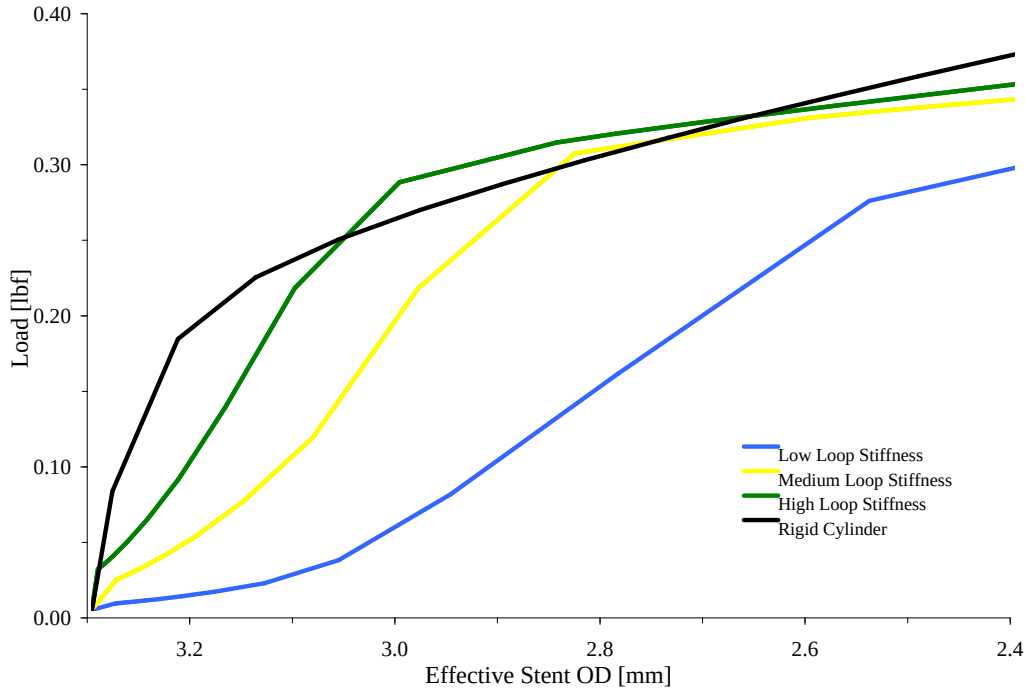

Figure 25: Force versus effective stent OD demonstrating the effects of loop strap material stiffness.

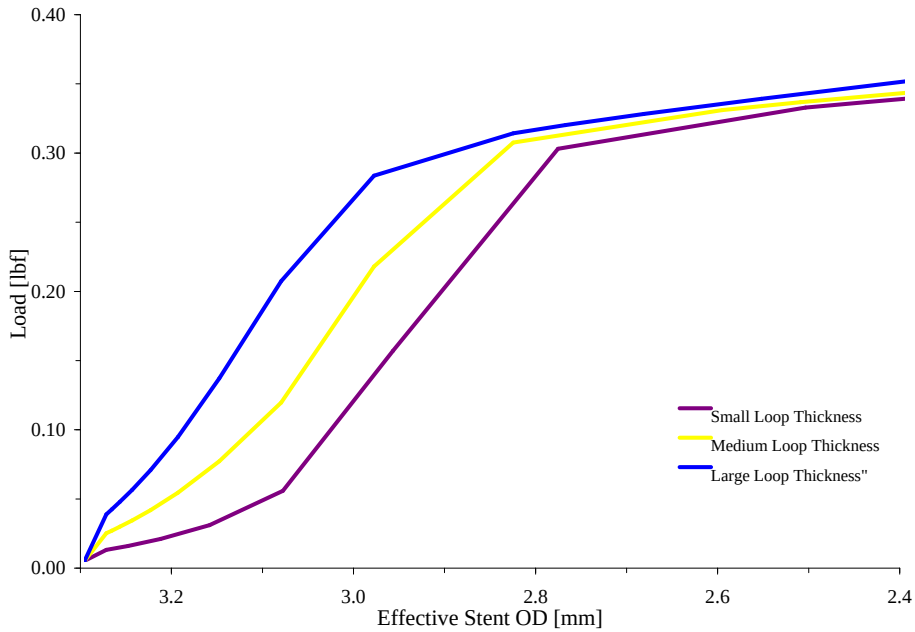

Figure 26: Force versus effective stent OD demonstrating the effects of loop strap thickness.

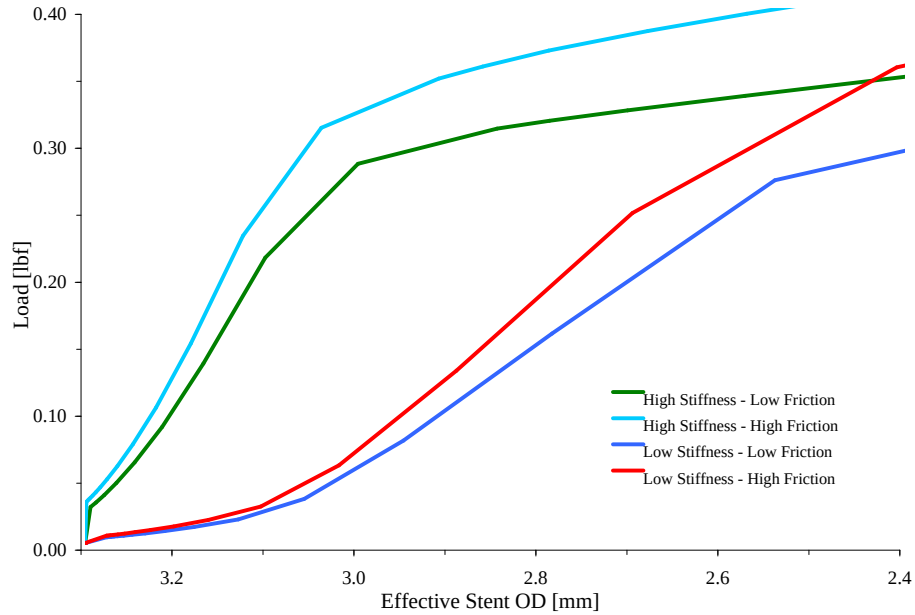

Figure 27: Force versus effective stent OD demonstrating the effects of friction.

5 Analysis Discussion

- The influence of friction increases as the loop test progresses due to increasing normal force between the loop strap and the stent.
- Loop strap compliance (both thickness and material stiffness) has the greatest influence at the start of the test during which time the loop compliance enables the loop to conform to the profile of the stent.
- The best fit representation to the Loop Test experimental results is shown in Figure 28 for Stent 2; however, a more detailed comparison between the numerical and experimental results will confirm/improve the correlation of key experimental parameters.
- Using the best fit representation to the Loop Test for Stent 2, a loop test simulation was performed on Stents 1 and 3 and the results of the three simulation are shown in Figure 29.

Additional Comments:

There are still many simplifications made in the Finite Element Analyses presented herein. There are additional considerations which were neglected and which may strongly influence the results:

- End effects of the loop strap as well as the stent.
- Asymmetry between the top and bottom halves of the stent including gravitational effects.
- Fixture flexure and friction between the loop strap and the sliders.

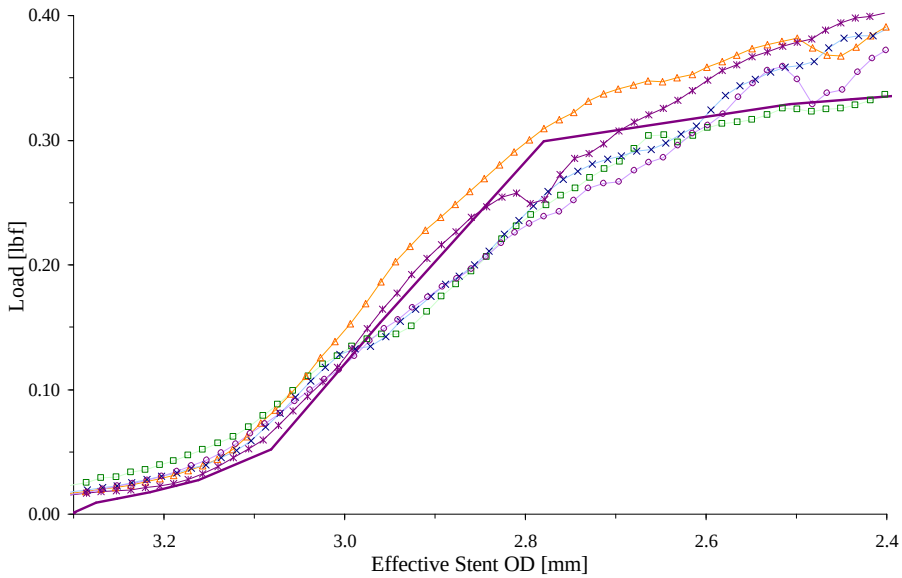

Figure 28: Best fit representation of the numerical simulation and experimental results for the Loop Test Method for Stent 2.

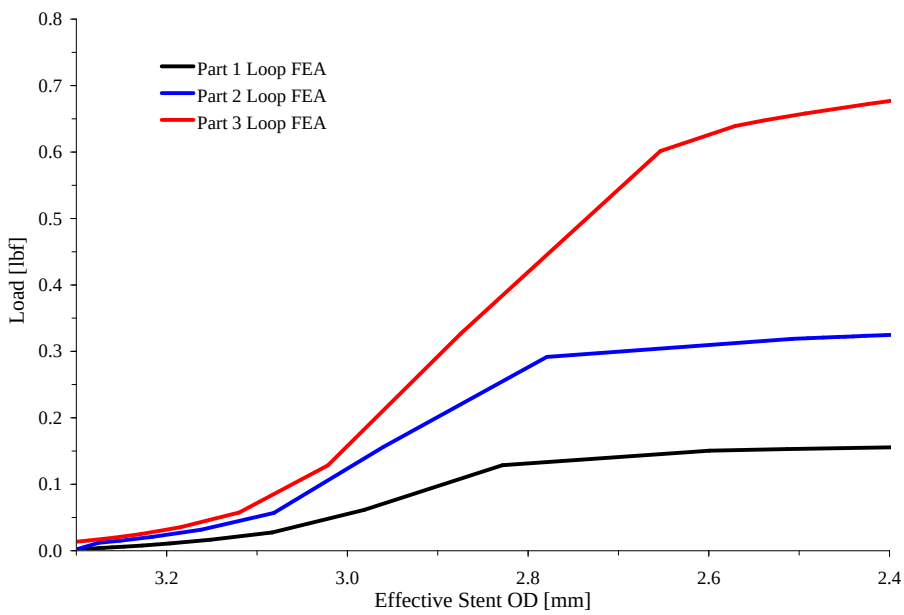

Figure 29: Best fit representations of the numerical simulations for Stents 1, 2, and 3.

6 Recommendations

- A similar analysis should be performed for the Concentric Cylinder Test Method to determine the sensitivity and impact of key experimental parameters.
- Comparisons between the two (and other?) test methods can be performed to evaluate the relative advantages/disadvantages of the different tests and determine conditions for obtaining valid results.
- The definition of radial stiffness for a stent needs to be further discussed in light of differences between in vitro and in vivo conditions.